



# PATTERNS OF THE SEISMIC GENERATION RATE DETECTED BY THE SOUTHERN CALIFORNIA SEISMIC NETWORK (SCSN)

M.D. Martínez<sup>(1)</sup>, X. Lana<sup>(2)</sup>

<sup>(1)</sup> Dept. Física Aplicada, Universitat Politècnica de Catalunya, Av. Diagonal, 649, 08028 Barcelona, Spain (dolors.martinez@upc.edu)

<sup>(2)</sup> Dept. Física i Enginyeria Nuclear, Universitat Politècnica de Catalunya, Av. Diagonal, 647, 08028 Barcelona, Spain (francisco.javier.lana@upc.edu)



## Objectives and Methodology

Several patterns of the seismic generation rate, *SGR*, of the seismic activity detected by the SCSN network are determined. *SGR* time series are derived from the SCSN catalogue (years 1981-2007) considering local magnitudes equaling to or exceeding 1.5, thus being assured magnitude completeness of the database. The characterization is based on six parameters:

1. An irregularity index, *Ilog*, based on entropy concepts
2. Time trend analysis, including time trends, *Slp*, and statistical significance, *Emk*
3. Autocorrelation and power spectrum contents
4. Cross-correlation and cross-power spectrum
5. Rescaled analysis and interpretation of the Hurst exponent, *H*, in terms of persistence, anti-persistence or randomness of *SGR*
6. The parameters of the statistical distribution of the seismic rates.

*SGR* series are obtained for the whole SCSN spatial domain, (32°-37°N) x (114°-122°W), and for cells of 1°x1° size within the SCSN domain. 23 cells of 1° x 1° depict high enough seismic activity to generate representative local *SGR* series, being possible to characterize interactions among cells, basically by means of cross-correlation and cross-power spectrum analysis. Parameters for cells containing 30 earthquakes, 3 out of them including the notable main shocks of *Landers* (L), *Northridge* (N), and *Hector Mine* (H), with seismic moment magnitudes, *M<sub>w</sub>*, of 7.3, 6.7 and 7.1 respectively, are revised. The six parameters are also computed for the aftershock areas of the three main shocks and specific periods of solely background seismic activity, removing the interference of aftershock activity and/or activity related to close seismic crisis. Thus patterns previous to and after a seismic crisis can be compared. The fitting of *SGR* to any statistical distribution is investigated, for the whole catalogue or for the four crises considered.

SCSN	<i>Ilog</i>	<i>Emk</i>	<i>Slp</i>	<i>H</i>	$\beta$
34.5°N 118.5°W	0.25	-4.80	-0.65	0.77	1.05
32.5°N 117.5°W	0.64	-8.66	-0.02	0.77	0.81
32.5°N 116.5°W	0.44	-1.45	-----	0.84	0.71
32.5°N 115.5°W	0.53	5.57	0.06	0.62	0.73
32.5°N 114.5°W	0.64	-10.37	-0.01	0.71	0.22
33.5°N 118.5°W	0.57	-10.45	-0.03	0.68	0.37
33.5°N 117.5°W	0.38	0.75	-----	0.81	0.57
33.5°N 116.5°W	0.29	-9.31	-0.18	0.80	0.86
33.5°N 115.5°W	0.74	-3.41	-0.02	0.64	0.35
33.5°N 114.5°W	0.41	-10.91	-0.02	0.97	1.37
34.5°N 119.5°W	0.68	-6.20	-0.01	0.66	0.07
34.5°N 118.5°W	0.42	-0.60	-----	0.67	0.41
34.5°N 117.5°W	0.30	-7.71	-0.07	0.73	0.40
34.5°N 116.5°W	0.33	2.49	0.06	0.78	1.18
35.5°N 121.5°W	0.62	-9.45	-0.01	0.69	0.42
35.5°N 120.5°W	0.73	-3.22	-0.01	0.78	0.50
35.5°N 119.5°W	0.76	-3.56	-0.01	0.65	0.34
35.5°N 118.5°W	0.39	-6.67	-0.05	0.73	1.19
35.5°N 117.5°W	0.38	-8.15	-0.10	0.73	0.80
35.5°N 116.5°W	0.68	-3.94	-----	0.76	1.08
36.5°N 121.5°W	0.65	-7.00	-0.01	0.78	0.46
35.5°N 120.5°W	0.59	-13.12	-0.04	0.83	0.87
35.5°N 118.5°W	0.78	-5.08	-0.02	0.70	0.33
35.5°N 117.5°W	0.59	4.62	0.04	0.74	0.55

Table 1. Parameters of the *SGR* series for left-, the whole SCSN domain (first row) and 23 cells of 1°x1° with notable seismic activity, and right-, the four seismic crisis. Red bold types identify time

trends (*Slp* given in *SGR*/months) with significant levels exceeding 99% and/or evident persistence (*H* exceeding 0.75), in agreement with the meaning of the Hurst exponent. Latitudes and longitudes represent coordinates of the seismic network centre and of the 23 cells.

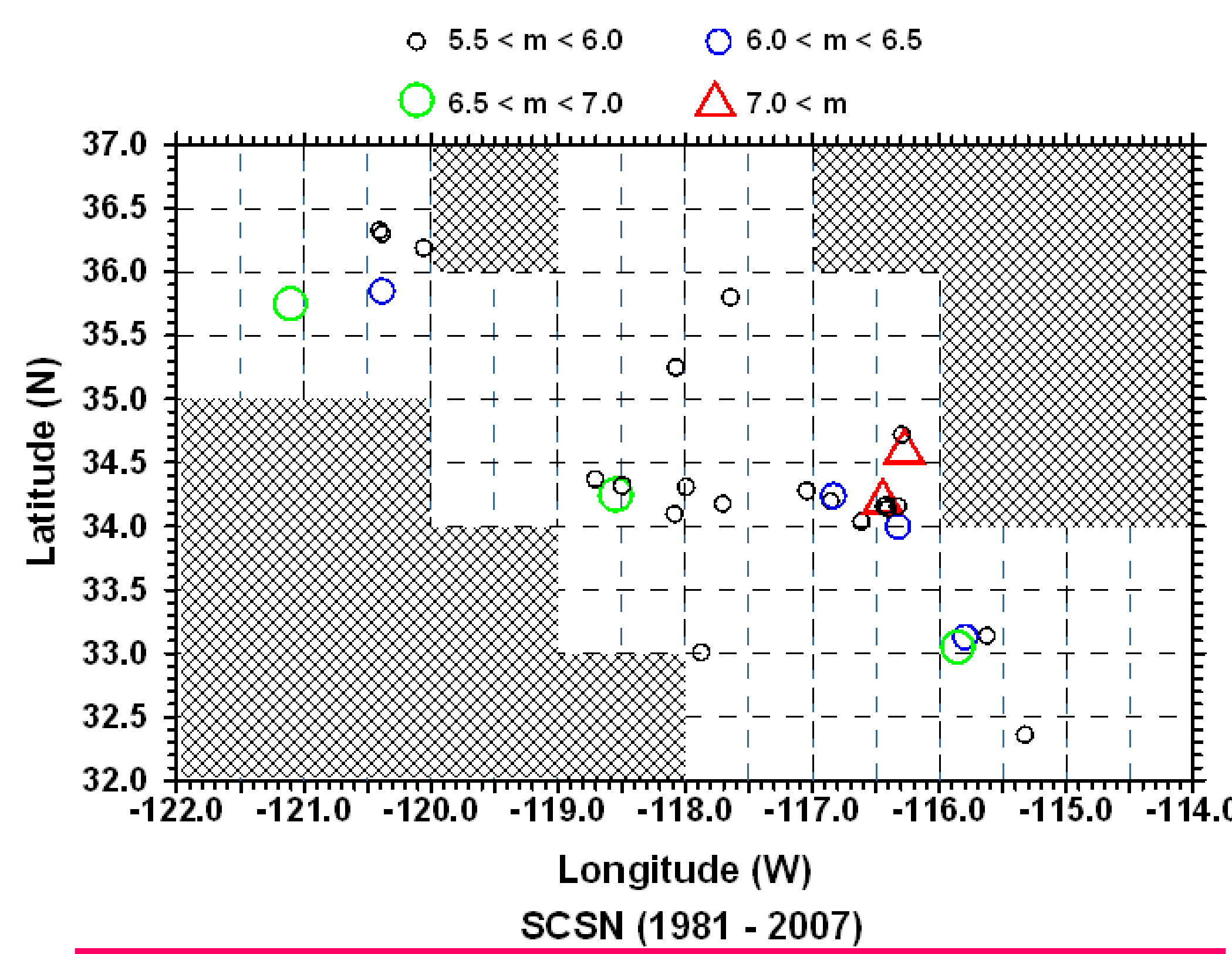


Fig. 1 Southern California analysed area (excepting shadow domains) and events equaling to or exceeding 5.5 magnitude

### Irregularity Index, *Ilog*

$$Ilog = [1/(N-1)] \sum_{i=1}^{N-1} LOG \{SGR(i+1)/SGR(i)\}$$

### Hurst exponent, *H*

*H* < 0.5, antipersistence; *H* ≈ 0.5, randomness; *H* >> 0.5, persistence

### Mann-Kendall statistic, *E<sub>MK</sub>*

|*E<sub>MK</sub>*| > 2.56 : time trend exceeding 99% significance level

### Generalised logistic distribution, *GLO*

$$F(x > SGR) = 1/[1 + exp(-\gamma)]$$

$$\gamma = -(1/\kappa) \log [1 - \kappa(x - \xi)/\alpha] ; \kappa \neq 0$$

### Power Law for the spectral amplitude *S(ω)* ~ ω<sup>-β</sup>

	$\kappa$	$\alpha$	$\xi$	$\Delta SGR$
SCSN	-0.54	154.4	564.4	277.0, ∞
LN	-0.66	84.25	264.5	136.8, ∞
NR	-0.76	8.81	27.1	15.4, ∞
HM	-0.71	68.35	159.1	62.8, ∞
SS	-0.48	2.95	5.5	0.65, ∞

Table 2. Parameters  $\kappa$ ,  $\alpha$  and  $\xi$  of the *GLO* distribution for the whole SCSN catalogue and the four seismic crises.  $\Delta SGR$  represents the range of *SGR* according to the theoretical *GLO* model.

HL	HN	HS	LN	LS	NS
1.18	0.84	1.02	0.83	1.02	0.67

Table 3. Parameter  $\beta$  of the power-law for cross-power spectra derived from pairs HL, HN, HS, LN, LS and NS

Cross-correlation					
HL	HN	HS	LN	LS	NS
0 (1.00)	18 (1.00)	137 (1.00)	18 (1.00)	137 (1.00)	119 (1.00)
87 (0.40)					

Autocorrelation			
L	N	H	S
1 (0.69)	1 (0.31)	1 (0.70)	1 (0.49)
			9 (0.26)

Table 4. Lags (in months) for which relevant peaks of auto- and cross-correlation are detected. Only normalized coefficients (within parentheses) exceeding 0.25 are included.

## MAIN RESULTS / CONCLUSIONS

- > Cells of 1°x1° are characterized by a high number of significant trends on *SGR* (99% of confidence and most of them negative). A notable number of significant time trends are related to persistence in agreement with the meaning of the Hurst exponent. All *SGR* series are free of randomness or anti-persistence.
- > The *SGR* (whole network) is characterized by a statistically significant (99%) negative trend and high persistence. The irregularity index is smaller than those derived for individual cells.
- > Changes in *SGR* due to different states of stresses before a main shock and along the aftershock process are suggested for the four seismic crises. It is a common feature that a stationary *SGR* level is achieved some time before finishing the assumed aftershock process.
- > When an aftershock area (partially) includes the domain corresponding to a previous main shock, its influence is manifested years after, although its aftershock activity could yet be assumed irrelevant or finished. An example could be the interaction Landers - Hector Mine.
- > This interaction, even at large distances, is also suggested observing cross-correlation plots for pairs of seismic crises, which depict peaks at lags ranging from 20 to 140 months.
- > Out of the four aftershock areas, only that from San Simeon exhibits *SGR* series with significant trend and persistence. For the rest of series, statistical significances are less than 95%.
- > A simple behavior has not been detected for periods of assumed "pure background seismic activity" free of the effects of main events. Although persistence is always quite evident, trends are statistically significant or not significant, without a common pattern. As a counterpart, irregularity is different for every domain but very similar for periods of "pure background seismic activity" belonging to the same aftershock area.
- > The analysis of pairs {*H*,  $\beta$ } for every cell, the whole SCSN and catalogues derived for the four aftershock areas suggest that *SGR* series for 15 out of 23 cells could be represented by a filtered fractional Gaussian noise, accomplishing  $H \approx (1+\beta)/2$ . *SGR* series corresponding to the spatial domain defined by Northridge crisis also accomplishes this relationship.
- > *SGR* series are quite well-fitted to a three-parameter Generalized Logistic distribution, for the whole SCSN and for the four aftershock areas considered.

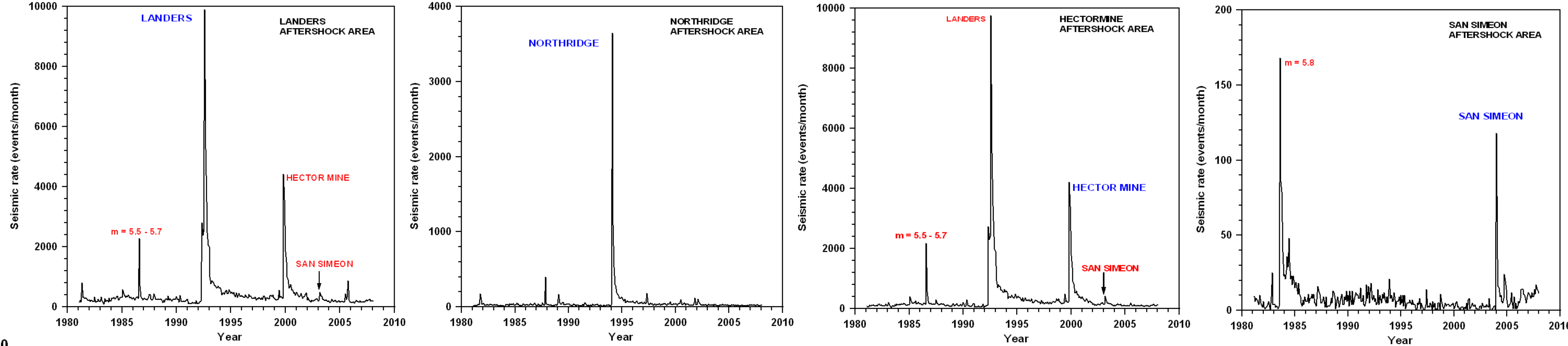


Fig. 2 Seismic generation rate for the aftershock areas of Landers, Northridge, Hector Mine and San Simeon

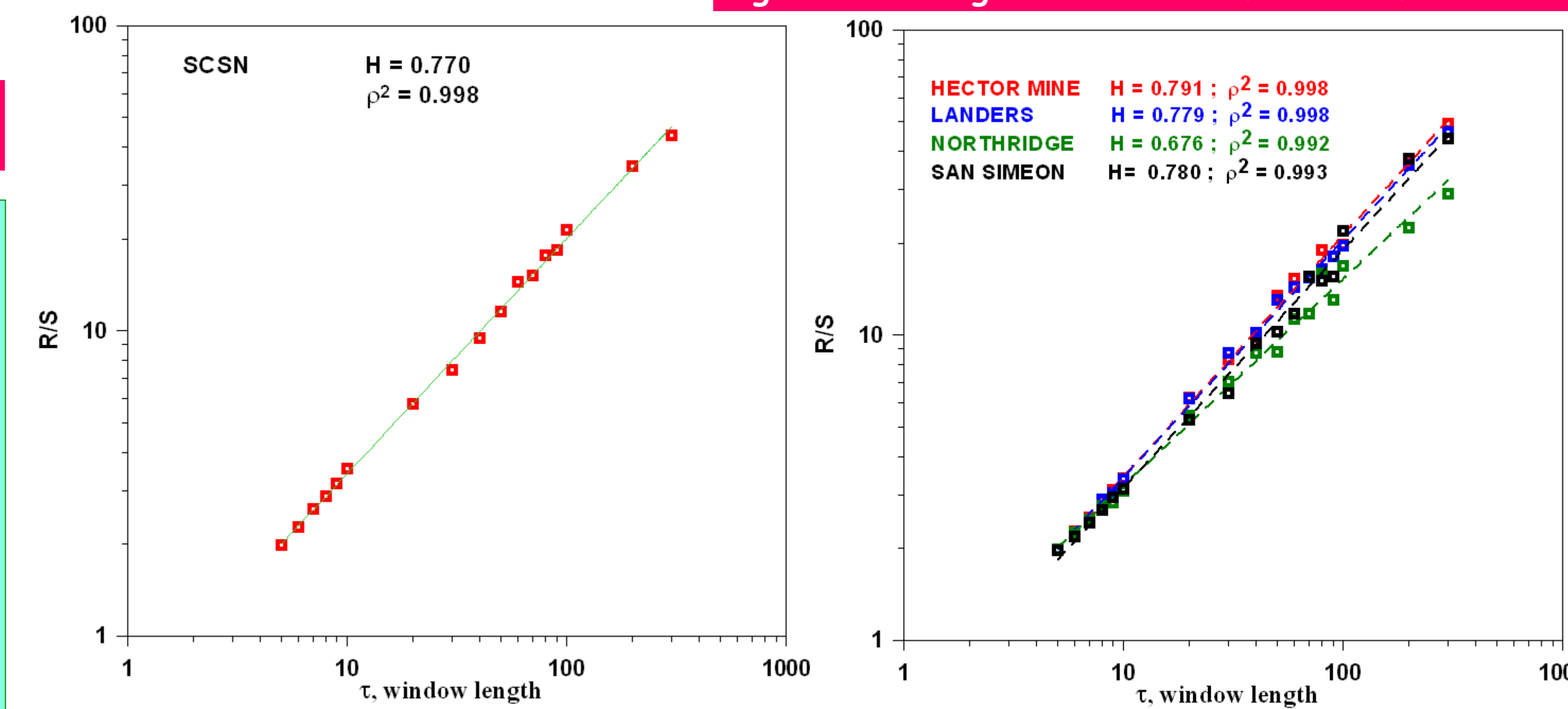


Fig. 3 Several examples of rescaled analysis for the SCSN catalogue and the four seismic crises

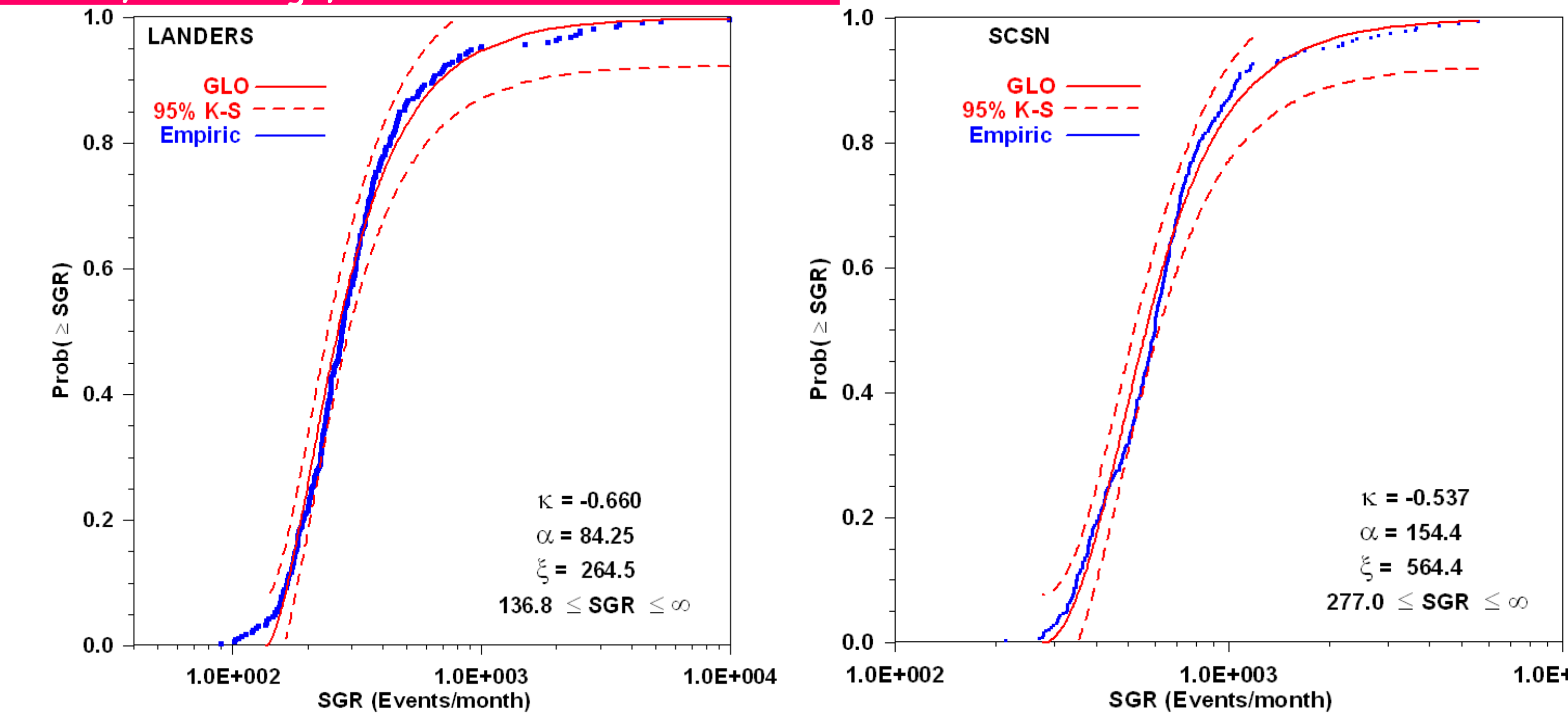


Fig. 3 GLO distribution for Landers aftershock area and the whole SCSN catalogue

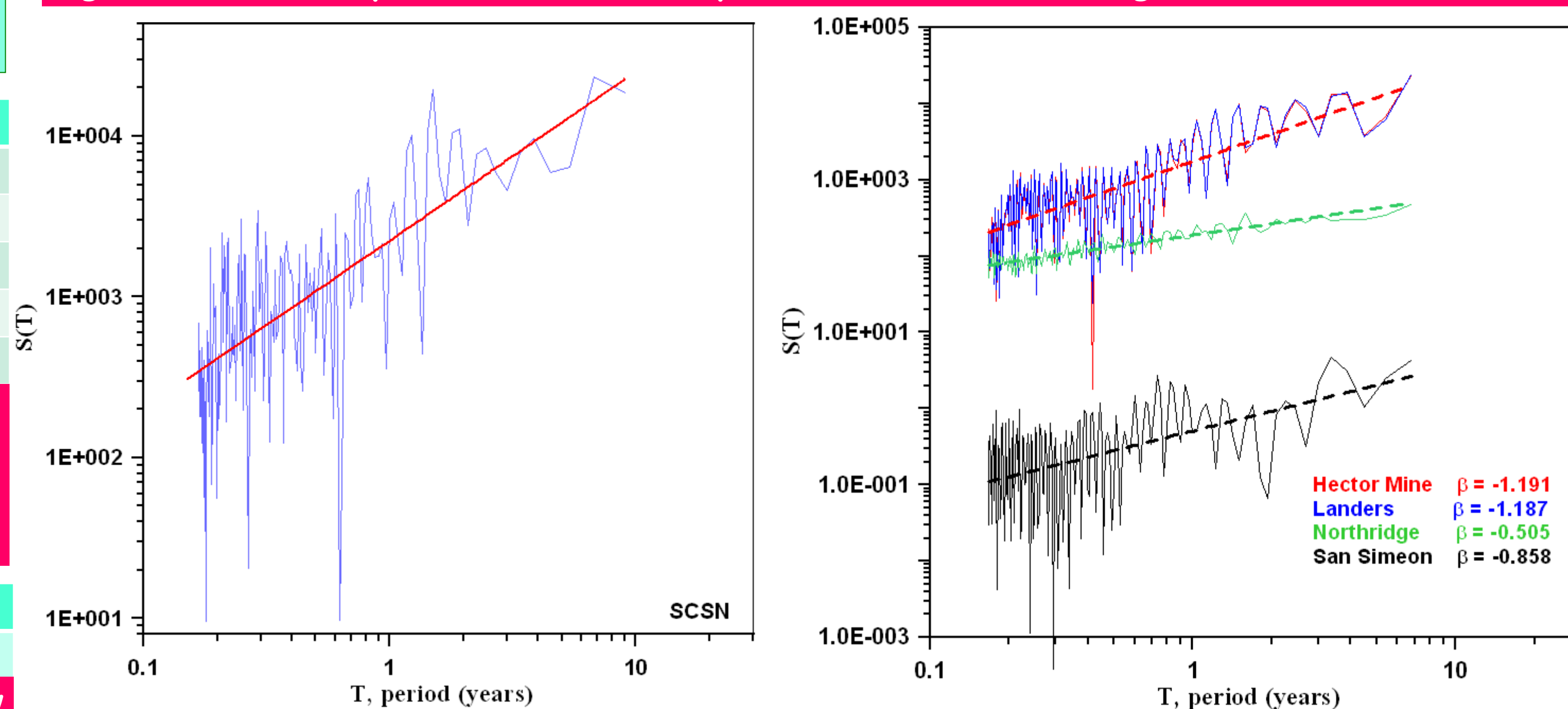


Fig. 4 Power spectra for the SCSN catalogue and the four seismic crises

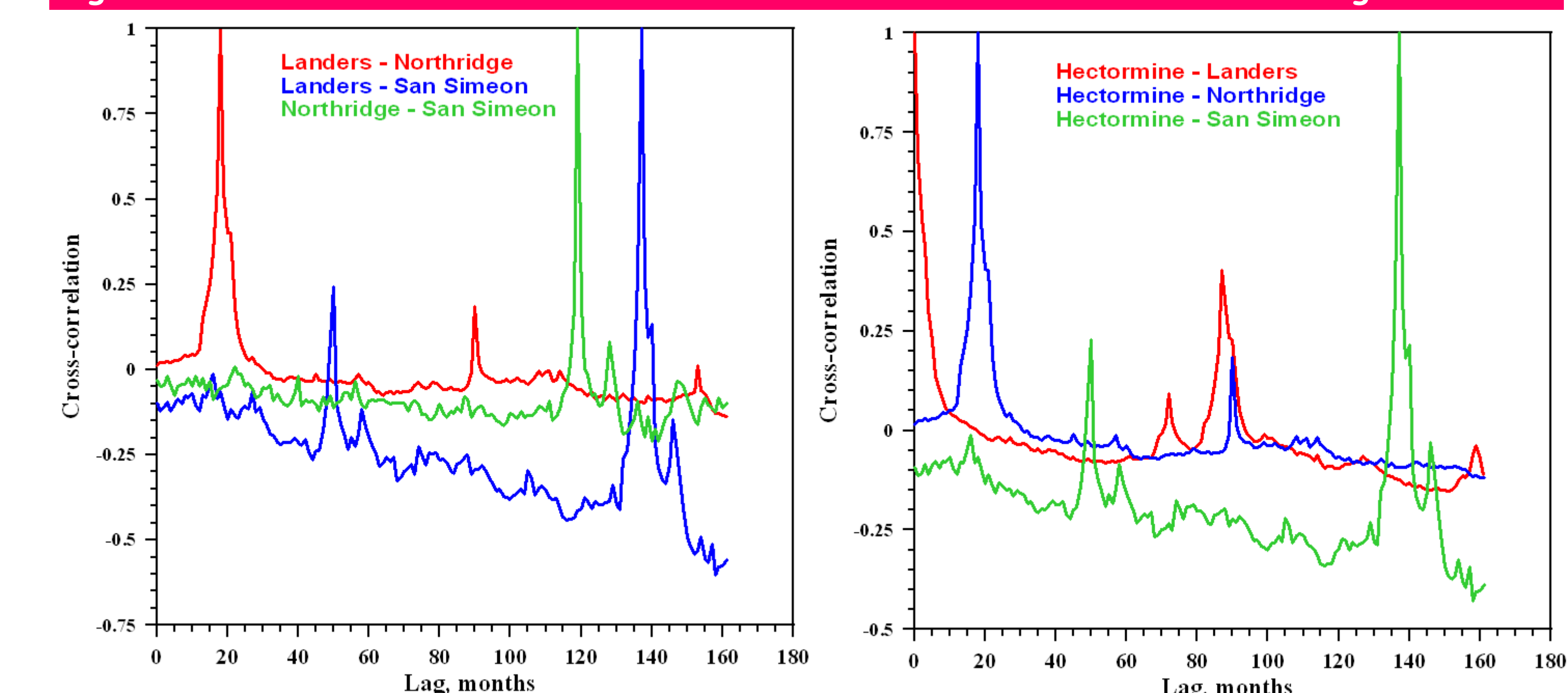


Fig. 5 Cross-correlation for pairs of seismic crisis

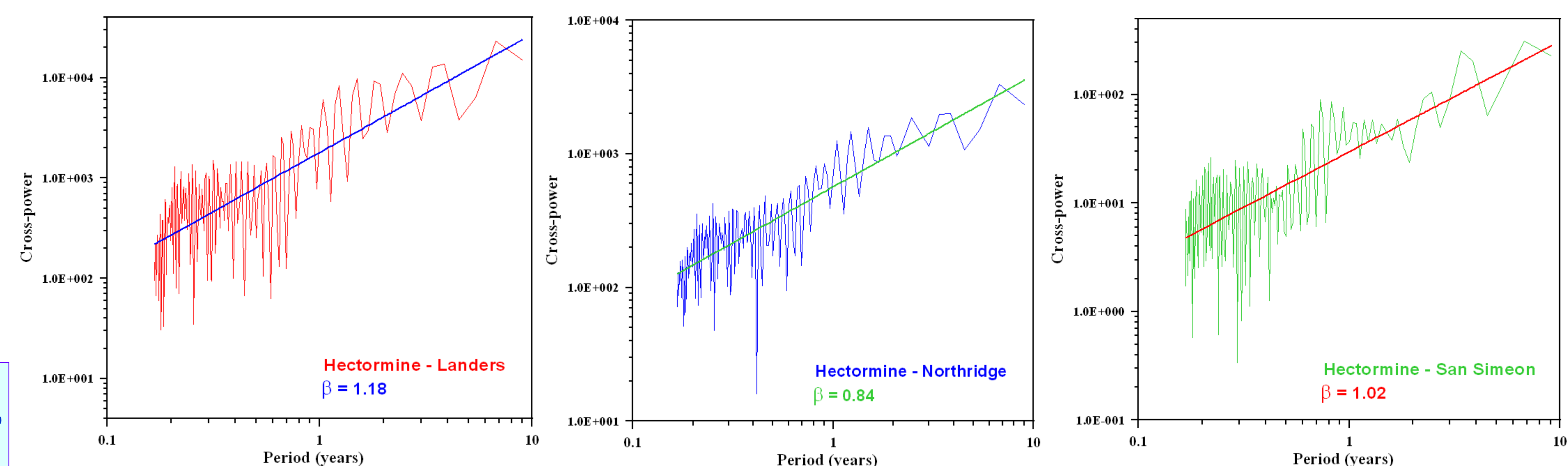


Fig. 6 Cross-power spectra for pairs HL, HN and HS

## REFERENCES

-Bottiglieri, M., Lippiello, E., Godano, C., de Arcangelis, L. (2009). Identification and spatiotemporal organization of aftershocks. *J. Geophys. Res.*, 114, B03303.

-Goltz, Ch. (1997). *Fractal and Chaotic Properties of Earthquakes*. Lecture Notes in Earth Sciences, vol. 77. Springer-Verlag, 178 pp.

-Hosking, J.R.M., Wallis, J.R. (1997). *Regional Frequency Analysis. An approach based on L-moments*. Cambridge University press, 224 pp.

-Shcherbakov, R., Turcotte, D.L., Rundle, J.R. (2005). *Aftershock statistics*. *Pure Appl. Geophys.*, 162, 1051-1076.

-Turcotte, D.L. (1997). *Fractal and Chaos in Geology and Geophysics* (2nd Edition). Cambridge University press, 398 pp.